Neurochemical Research (2023) 48:658–670
https://doi.org/10.1007/s11064-022-03791-x

ORIGINAL PAPER

POU Domain Class 2 Transcription Factor 2 Inhibits Ferroptosis in Cerebral Ischemia Reperfusion Injury by Activating Sestrin2

Jinghui Yang[1] · Qian Guo[2] · Lu Wang[2] · Shan Yu[2]

Received: 14 April 2022 / Revised: 12 May 2022 / Accepted: 12 October 2022 / Published online: 28 October 2022

Abstract

Cerebral ischemia reperfusion injury (CIRI) is the commonest cause of brain dysfunction. Up-regulation of POU domain class 2 transcription factor 2 (POU2F2) has been reported in patients with cerebral ischemia, while the role of POU2F2 in CIRI remains elusive. Middle cerebral artery occlusion/reperfusion (MCAO/R) in mice and oxygen and glucose deprivation/reperfusion (OGD/R) in mouse primary cortical neurons were used as models of CIRI injury in vivo and in vitro. Lentivirus-mediated POU2F2 knockdown further impaired CIRI induced by MCAO/R in mice, which was accompanied by increased-neurological deficits, cerebral infarct volume and neuronal loss. Our evidence suggested that POU2F2 deficiency deteriorated oxidative stress and ferroptosis according to the phenomenon such as the abatement of SOD, GSH, glutathione peroxidase 4 (GPX4) activity and accumulation of ROS, lipid ROS, 4-hydroxynonenal (4-HNE) and MDA. In vivo, primary cortical neurons with POU2F2 knockdown also showed worse neuronal damage, oxidative stress and ferroptosis. Sestrin2 (Sesn2) was reported as a neuroprotection gene and involved in ferroptosis mechanism. Up-regulation of Sesn2 was observed in the ischemic penumbra and OGD/R-induced neuronal cells. Further, we proved that POU2F2, as a transcription factor, could bind to Sesn2 promoter and positively regulate its expression. Sesn2 overexpression relieved oxidative stress and ferroptosis induced by POU2F2 knockdown in OGD/R-treated neurons. This research demonstrated that CIRI induced a compensatory increase of POU2F2 and Sesn2. Down-regulated POU2F2 exacerbated CIRI through the acceleration of oxidative stress and ferroptosis possibly by decreasing Sesn2 expression, which offers new sights into therapeutic mechanisms for CIRI.

Keywords POU2F2 · Sesn2 · Oxidative stress · Ferroptosis · Cerebral ischemia reperfusion

Introduction

Cerebrovascular disease is a common clinical condition that seriously threatens human health and life. With the increase in population aging, the morbidity, disability and mortality rate of cerebrovascular events are increasing through the year [1, 2]. Among them, ischemic cerebrovascular disease constitutes a significant proportion and is the most harmful [3]. The principal treatment for cerebral ischemia is to restore cerebral perfusion and maintain blood flow [4]. Upon the restoration of blood flow, oxygen returnes to the ischemic areas of the brain to rescue and rebuild neurons [5]. However, ischemia reperfusion can elicit rapid cascade response damage to neuronal cells, exacerbate pathological damage to ischemic tissue, and eventually induce apoptosis or necrosis of neuronal cells, that is cerebral ischemia reperfusion injury (CIRI) [6, 7]. Over the years, basic experiments have revealed that the potential molecular mechanisms of CIRI involved numerous pathological processes such as oxidative stress, apoptosis, inflammation, autophagy and necrosis [8, 9]. Currently, it is difficult to prevent further damage caused by reperfusion, and effective preventive measures have not been established.

Ferroptosis is a newly identified form of cell death proposed by Dixon et al. in 2012 [10], which differs from other modes of death such as apoptosis, necroptosis and autophagy in terms of morphological and biochemical characteristics and regulatory mechanisms. Ferroptosis is a regulated-form of cell death that is driven by iron-mediated reactive oxygen

✉ Shan Yu
yushan1101@jlu.edu.cn

[1] Department of Hepatobiliary and Pancreatic Surgery, China-Japan Union Hospital of Jilin University, Changchun, Jilin Province, China

[2] Department of Neurology, China-Japan Union Hospital of Jilin University, No. 126, Xiantai Street, Changchun, Jilin Province, China

species (ROS) production followed by lipid peroxidation. The abnormal accumulation of lipid hydroperoxides in the presence of ferrous iron leads to membrane disruption and irreversible cell death [11]. The biochemical mechanism of ferroptosis is the combination of iron-catalyzed formation of lipid ROS with depletion of glutathione (GSH) or deactivation of the lipid repair enzyme glutathione peroxidase 4 (GPX4) [12]. GPX4 is a GSH-dependent selenoenzyme that prevents ferroptosis by reducing deleterious lipid hydroperoxides to harmless lipid alcohols. Proper regulation of GSH biosynthesis and GPX4 level is the key cellular process for the inhibition of ferroptosis. A large body of researches have demonstrated that ferroptosis is involved in multiple brain diseases including neurological conditions, IR injury, stroke and intracerebral hemorrhage [12, 13]. Blocking ferroptosis is proposed as a promising therapeutic strategy for the treatment of those above devastating diseases and has shown positive results [14].

Sestrin2 (Sesn2) is a highly conserved protein during evolution that is induced by stress conditions including oxidative stress, DNA repair and hypoxia [17]. Sesn2 has protective effects on physiological and pathological states, mainly through the regulation of oxidative stress, endoplasmic reticulum stress, autophagy, and metabolic and inflammatory responses [18]. It has been demonstrated that Sesn2 was up-regulated in cerebral ischemia or IR animal models, and that Sesn2 overexpression alleviated ischemia or IR-induced brain injury, while inhibition of Sesn2 exacerbated brain injury [19]. In published studies, the biological function of Sesn2 in CIRI has been reported to exacerbate CIRI via uncontrolled oxidative stress and mitochondrial dysfunction [20]. In addition, the cytoprotective effects of Sesn2 has been reported in ferroptosis-induced tissue injury [21], suggesting the possible role of Sesn2 on ferroptosis in CIRI.

POU domain class 2 transcription factor 2/Octamer-2 (POU2F2/OCT-2) is one of the members of POU domain family that utilizes POU-specific structural domain to bind to DNA and active transcription [22]. POU2F2 initially is regarded as B-cell-restrict transcription factor that regulates B cell proliferation and differentiation by binding to the immunoglobulin gene promoter [23]. Meanwhile, it also has been shown to be expressed in neuronal cells [24], and Latchman et al. [25] reported that POU2F2 might play a crucial role in the development of the central nervous system. Recently, a study identified that POU2F2 was highly expressed in a rat model of cerebral ischemia and found to be involved in reducing ischemic-mediated neuronal injury [26]. It has been suggested to participate in the neuronal basic cellular functions (apoptosis, survival and growth), neuronal vascular development, neuronal inflammation and cell death via interaction with multiple transcription factors such as ETS [27], MEF [28], and NF-kB [29]. By using online prediction website, we found potential binding sites between POU2F2 and Sesn2 promoter. However, their combination and regulatory relationship in CIRI have not been reported. In our research, we aim to unveil the actual role and potential mechanism of POU2F2 in CIRI as well as to examine the link between POU2F2 and Sesn2.

Methods

Lentivirus Production

Lentivirus-mediated POU2F2 knockdown or Sesn2 overexpression was conducted as previously described [30] [PMID: 33,037,113]. The specific POU2F2 short hairpin RNA (shRNA) and its negative control sequences were synthesized by General Biosystems (Anhui, China) and cloned into pLVX-shRNA1 lentiviral vector (Fenghui Biotechnology, Hunan, China, CAS: BR004). The plasmid of Sesn2 overexpression was also constructed by General Biosystems and cloned into pLVX-IRES-puro lentiviral vector (Fenghui Biotechnology, Hunan, China, CAS: BR025).

Lentiviruses were generated by cotransfection of HEK-293T cells (Zhong Qiao Xin Zhou Biotechnology Co., Ltd., Shanghai, China) with lentiviral plasmid (shPOU2F2 plasmid or Sesn2 overexpression plasmid) and two helper plasmids, psPAX2 and pmD2.G (Fenghui Biotechnology, Hunan, China, CAS: BR004), using Lipofectamine 3000 (Invitrogen, Carlsbad, CA, USA). The medium was replaced 6 h transduction with complete growth media.

The virus-containing medium was harvested 48 h after cultivation, centrifuged at 1000 rpm for 10 min and filtered at 0.45 μm filter. The viral titer was determined by RT-qPCR. Lentivirus particles were frozen at -80℃ for further use.

Animals

Male C57BL/6 mice were purchased from Beijing Hua Fukang Biotechnology Co., Ltd. (Beijing, China). Mice for the experiment were 10 to 12 weeks old. Mouse husbandry and experiments were conducted under the ethical guideline of the Animal Welfare and Research Ethics Committee of Jilin University. Mice were exposed to a controlled-environment: 12: 12 h dark/light cycle, 45–55% humidity and 21–23℃. All mice were allowed free access to water and pelleted ad libitum. Mice were accustomed to the environment for 7 days prior to experiment.

Experiment 1: CIR was induced by middle cerebral artery occlusion/reperfusion (MCAO/R) as described previously [31]. Briefly, during surgery, the body temperature of anesthetized mice was maintained at 37-37.5℃ using a heating pad. A midline ventral cervical incision was made, and a nylon suture was inserted into the internal carotid artery (6 mm from

the internal carotid/pterygopalatine artery bifurcation) through the stump of the external carotid artery for unilateral MCAO. After 60 min of MCAO, the suture was withdrawn to allow reperfusion. Animals survived for 6 h, 24 h, 48 h, 72 h and 7 days. The ischemic penumbra region (cortex) was collected for further analysis.

Experiment 2: A total of 2 μL LV-shPOU2F2 or LV-shNC lentiviruses (5×10^8 TU/mL) were slowly injected into ipsilateral lateral ventricles (coordinates: anteroposterior-0.3 mm, mediolateral-1.0 mm, dorsoventral-2.2 mm to the bregma). Sham or MCAO/R surgery was carried out after 72 h lentivirus injection. After 72 h reperfusion, neurological deficit was confirmed and scored as follows: 0, no deficits; 1, forelimb weakness and torso turning to the ipsilateral side when held by tail; 2, circling to affected side; 3, unable to bear weight on affected side; and 4, no spontaneous locomotor activity or barrel rolling [31]. Mice were then sacrificed, and the brain tissues were collected. The inhibitory effect of lentiviral shRNA on POU2F2 expression was analyzed by RT-qPCR.

Cell Culture and Treatment

Primary cortical neurons were dissociated from C57BL/6 mice as previously described [32]. The cerebral cortex was minced into small pieces and then digested in 0.125% trypsin for 15 min. The single cell suspension was cultured in Neurobasal medium (Gibco Life Technologies, Grand Island, NY, USA) containing 3% B27 (Gibco Life Technologies, Grand Island, NY, USA) and 0.5 mM glutamine (Yuanye Bio-Technology Co., Ltd., Shanghai, China). Primary cells were identified by a light microscope. Cells were seeded on poly-L-lysine hydrobromide (Yuanye Bio-Technology Co., Ltd., Shanghai, China)–coated 6, 24 or 96-well plate for further experiments.

Oxygen-glucose deprivation and reoxygenation (OGD/R) procedure was performed to mimic CIR in vitro [33]. Primary cortical neurons were cultured in glucose-free Dulbecco modified Eagle medium (DMEM) medium (Gibco Life Technologies, Grand Island, NY, USA) and hypoxic conditions with 5% CO_2 / 95% N_2 for 4 h to establish OGD conditions, followed by incubation in normal DMEN medium under normoxic conditions for 24 h as OGD/R.

Primary cortical neuron were co-cultured with lentiviral fluid (POU2F2 knockdown and/or Sesn2 overexpression) at the multiplicity of infection (MOI) of 5. The transduction efficiency was evaluated by RT-qPCR and western blot. After transduction for 48 h, cells were harvested for OGD/R treatment.

2,3,5-Triphenyltetrazolium Chloride (TTC) Staining and Nissl Staining

Frozen brain tissues were cut into sections and then incubated with 2% TTC in 0.01 M phosphate buffer solution for 15 min at 37℃. Infarcted brain tissues were unstained (white) and non-infarcted areas were in red. The staining results were photographed.

For Nissl staining, brain sections were incubated with 0.5% cresyl violet (Sinopharm Chemical Regent Co., Ltd., Beijing, China) for 10 min under room temperature, and differentiated in 95% ethanol with 0.25% glacial acetic acid. The sections were then dehydrated through graded ethanol and cleared in xylene. The sections were viewed by microscope (Olympus, Tokyo, Japan).

MTT Assay

Primary cells in 96-well plates were incubated with 3-(4, 5-dimethylthiazol-2-yl)-2, 5-diphenyltetrazolium bromide (MTT) (Beyotime Biotechnology, Shanghai, China) for 4 h followed by 3 h incubation with Formazan solvent. Cell viability was determined using microplate reader (BioTek Instruments, Inc., Winooski, VT, USA), and MTT optical density (OD) value at 570 nm was recorded.

IF and Immunohistochemistry (IHC) Staining

Cells were fixed in 4% paraformaldehyde and permeabilized with 0.1% Triton X-100. Mouse brain tissue sections were paraffin-embedded and sectioned into 5 μm slides. Sodium citrate buffer was used for antigen repair. Non-specific binding was blocked in 1% bovine serum albumin (BSA). Primary antibodies were incubated overnight at 4℃ (POU2F2, Affbiotech, Changzhou, China; NeuN, Abcam, Cambridge, UK; Sesn2, Proteintech Group, Inc., Wuhan, China). After washing in PBS three times, cells or tissue slides were incubated with goat-anti-rabbit IgG labeled with FITC (Abcam, Cambridge, UK) and/or goat-anti-mouse IgG labeled with Cy3 (Invitrogen, Carlsbad, CA, USA). For dual-immunofluorescence, two primary antibodies and two secondary antibodies were co incubated. Nuclei were stained with 4', 6-diamidino-2-phenylindole (DAPI) (Aladdin regents Co. Ltd., Shanghai, China) solution. Immunofluorescent images were captured with microscope (Olympus, Tokyo, Japan).

Tissue sections for IHC were treated with 3% hydrogen peroxide to block endogenous peroxidases and blocked for 15 min in 1% BSA. IHC was performed with 4-hydroxynonenal (4-HNE) antibody (R&D systems, MPLS, MN, USA) and corresponding horseradish peroxidase (HRP)-conjugated secondary antibody (ThermoFisher Scientific,

Pittsburgh, PA, USA). Slides were revealed using 3, 3′-diaminobenxidine (DAB) (Maxinm Biotech, Fuzhou, China), and were counterstained with hematoxylin (Solarbio, Beijing, China) for visualization using light microscopy (Olympus, Tokyo, Japan).

ROS and Lipid ROS Detection

ROS detection in the penumbra area of ischemic cortex was performed using ROS detection kit (BestBio, Shanghai, China). Briefly, 10 μm slides were incubated with reaction solutions for 30 min at 37℃ and sealed with anti-fluorescence-attenuating sealer (Solarbio Science & Technology, Co., Ltd., Beijing, China). Intracellular ROS production was detected by 2, 7-dichlorofluorescein diacetate (DCFH-DA) (Solarbio Science & Technology, Co., Ltd., Beijing, China) according to the manufacturers' protocol. Cells were stained with C11-BODIPY581/591 probe (Maokang Biotechnology Co., Ltd., Shanghai, China) for 30 min to measure the levels of intracellular lipid ROS. ROS and lipid ROS production levels were measured by detecting fluorescence intensity under microscopy (Olympus, Tokyo, Japan).

RT-qPCR

TRIpure reagent (BioTeke Corporation, Beijing, China) was used to extract total RNA from brain tissues or primary cells, and the extracted RNA was reversely transcribed into cDNA using BeyoRT II M-MLV reverse transcriptase (Beyotime Biotechnology, Shanghai, China). RT-qPCR was performed on Exicycler 96 (Bioneer Corporation, Daejeon, Korea) using SYBR Green PCR master Mix (Solarbio, Beijing, China). Housekeeping gene β-actin was used for normalization of data before the calculation was performed with the $2^{-\Delta\Delta Ct}$ method. Primer sequences (forward and reverse, respectively) were exhibited as follows: POU2F2 (5′-CCA CAG GCA CAG CAG AGT C-3′; 5′-GAA GCG GGA AAT GGT CGT-3′) and Sesn2 (5′-GGT CCT GCT TAC CCA CTG CC-3′; 5′-GCT GCC TCA TGC GTT CCA TC-3′).

Western Blot

Total proteins from brain tissues and primary neuronal cells were extracted using RIPA lysis buffer, and then loaded on 10% or 15% acrylamide gel for electrophoresis. Proteins were transferred onto polyvinylidene difluoride membranes (PVDF) membranes (Thermo Scientific, Pittsburgh, PA, USA), and then incubated with specific primary antibodies (POU2F2, 1:1000, Affbiotech, Changzhou, China; Sesn2, 1:1000, Abcam, MA, USA; GPX4, 1:500, ABclonal Technology, Wuhan, China; β-actin, 1:2000, Proteintech Group, Inc., Wuhan, China) followed by HRP-conjugated goat-anti-mouse or goat-anti-rabbit secondary antibodies (Proteintech Group, Inc., Wuhan, China). Protein blots were visualized using enhanced chemiluminescence (ECL) detection reagent (7 Sea Pharmtech, Shanghai, China). The optical density of each protein blots were analyzed by Gel-Pro-Analyzer software. The quantification of each protein was performed as the optical density value ratio of the target bands to the internal control.

Dual-luciferase Assay System

To examine whether POU2F2 directly binds to Sesn2 promoter region, dual-luciferase reporter assay was performed using HEK-293T cells. The pGL3 luciferase reporter vector was utilized to construct reporter plasmid with different segments of Sesn2 promotor. For dual-luciferase plasmid transfection, 1.5 μL Lipofectamine 3000 was mixed with 25μL opti-MEM, and 0.5 μg plasmid, 1 μL Lipofectamine 3000 were mixed with 25μL opti-MEM. The two mixes were combined and incubated for 15 min under room temperature. Subsequently, the HEK-293T cells were seeded into 24-well plates and transfected with the combination of the mixture. After 48 h transfection, firefly and renilla luciferase activity were measured using Dual-Luciferase Reporter Assay Kit (KeyGEN, Nanjing, China) following manufacturer's instructions with a microplate reader. The firefly luciferase activities were normalized with respect to renilla luciferase activities.

Chromatin Immunoprecipitation (ChIP) Assay

ChIP assay was performed using ChIP assay kit (Wanlei Biotechnology Co., Ltd., Shenyang, China) according to the instruction manual. Primary cells were cross-linked by 1% formaldehyde for 10 min and quenched by glycine (0.125 M). The protein-bound chromatin was fragmented by sonication and harvested by centrifugation. The supernatant was incubated with anti-POU2F2 overnight at 4℃. Antibodies complexes were precipitated by protein A/G beads and then washed through an array of buffer solutions. Samples were de-crosslinked at 65℃ overnight followed by RNase A and proteinase K treatment. The DNA was harvested by DNA Gel Extraction Kit (Wanlei Biotechnology Co., Ltd., Shenyang, China) and analyzed by PCR. ChIP PCR products were loaded into 2.5% agarose gel and visualized by gold view nucleic acid dye, and then electrophoresis was conducted. The electrophoresis gels were then photographed by gel imaging system. List of primers used in ChIP assay: Sesn2 (5′-AGT CCC TCC AGG AAC TGG AAA G-3′; 5′-AGG GAG GTG TCG GCT CCG CCT-3′).

Oxidative Stress Level and Cytotoxicity Assay

The assay was performed according to Liu et al [34]. Malondialdehyde (MDA) content, superoxide dismutase (SOD) activity, glutathione (GSH) activity and lactate dehydrogenase (LDH) release were detected and calculated using MDA assay kit, GSH assay kit, SOD assay kit, and LDH activity assay kit from Jiancheng Bioengineering Institute (Nanjing, China) and Wanlei Biotechnology Co., Ltd. (Shenyang, China) respectively, following manufacturer' protocols. The MDA, SOD and GSH results were normalized relative to the concentration of total protein measured by BCA kit.

Statistic Analysis

Data were exhibited as mean ± standard deviation (SD). Data analysis was performed using Graphpad 8.0 software (GraphPad Prism, San Diego, CA, USA). In our study, Two tailed t-test (t-test) was used to analyze a difference between two groups, and One-way ANOVA with Tukey post hoc test was used among multiple groups. Analysis of variance differences was deemed significant when P values < 0.05. All experiments were performed three or more times independently under the same or similar conditions, unless otherwise stated.

Results

Depletion of POU2F2 Aggravated MCAO/R-induced Brain Injury in Mice

As shown in Fig. 1B, MCAO/R surgery significantly increased POU2F2 transcription and post-transcription levels in the cortical ischemic penumbra areas of mice after 72 h and 7 days of reperfusion. Based on POU2F2 expression, reperfusion for 72 h was chosen to establish an in vivo model of CIRI. Double immunofluorescent staining proved the decreased-neuronal nuclei (NeuN) immunoreactivity and increased-POU2F2 immunoreactivity in penumbra after 72 h reperfusion (Fig. 1C). Further, POU2F2 was silenced with lentiviral constructs. RT-pPCR and Western blot results revealed the decreased POU2F2 and Sesn2 expression in the ischemic penumbra of POU2F2-knockdown mice (Fig. 1D–F). The neurological deficit scores were investigated of these mice. MCAO/R induced pronounced neurological function impairment, whereas POU2F2 knockdown showed the worse neurological scores (Fig. 1G). Results shown that the ischemic cortical infarct volume was increased (Fig. 1H) in brain after MCAO/R, and POU2F2 knockdown led to further increases in infarct volume (Fig. 1H). As shown in Fig. 1I, cells positive for Nissl staining had contracted cell bodies with shrunken and pyknotic nuclei and were sparsely distributed. This phenomenon was pronounced in POU2F2-deficient mice, which exhibited severe neuronal damage in the ischemic penumbra (Fig. 1I). These data suggested that POU2F2 deficiency exacerbated IR-induced brain damage.

POU2F2 Knockdown Aggravated Neural Oxidative Stress and Ferroptosis Induced by MCAO/R

To determine the effect of POU2F2 on oxidative stress, ROS and SOD were determined as indicators of oxidative stress. As the results showed that the ROS production (Fig. 2A) and SOD activity (Fig. 2D) were significantly increased induced by MCAO/R compared to controlled-mice. Besides, 4-HNE expression (Fig. 2B) and MDA content (Fig. 2 C) were significantly increased after MCAO/R surgery compared with sham-operated mice, with POU2F2 deficiency leading to an even greater increase in both features compared with its negative control. Oxidative stress and lipid peroxidation are thought to be two important events in triggering ferroptosis [35]. Decreased GSH is a key factor of ferroptosis-mediated cell death, which is also characterized by reduced lipid repair enzyme GPX4. Results shown that POU2F2 knockdown exacerbated GHS activity (Fig. 2E) and negative regulator GPX4 expression levels (Fig. 2 F) in CIR mice compared to controlled-mice, suggesting the possible involvement of ferroptosis in POU2F2 knockdown-induced neuronal damage.

Knockdown of POU2F2 Exacerbated Neuronal Impairment and Aggravated Oxidative Stress and Ferroptosis in OGD/R-Treated Primary Neurons

To further confirm the involvement of POU2F2 in CIRI, we prepared primary cortical neurons from C57BL/6 mice and then identified under light microscopy. The primary cells were exposed to OGD/R to mimic ischemic injury in vivo. The expression of POU2F2 and Sesn2 was detected by Western blot (Fig. 3A) and RT-qPCR (Fig. 3B). Our results shown that POU2F2 and Sesn2 expression was highly expressed in OGD/R-treated primary cortical neurons compared to cells under normal conditions (Fig. 3A, B). Subsequently, shRNA lentivirus were transduced into cells to knockdown POU2F2 expression, and RT-qPCR was performed to verify the transduction efficiency (Fig. 3C). Primary cortical neurons with or without POU2F2 knockdown further were exposed to OGD/R. POU2F2 knockdown expression remarkably decreased elevated-POU2F2 levels stimulated by OGD/R (Fig. 3D) compared with control cells. Compared POU2F2 silencing to control cells, POU2F2-silenced primary neurons were more susceptible to OGD/R-induced cell death, as demonstrated by decreased cell survival rate (Fig. 3E) and

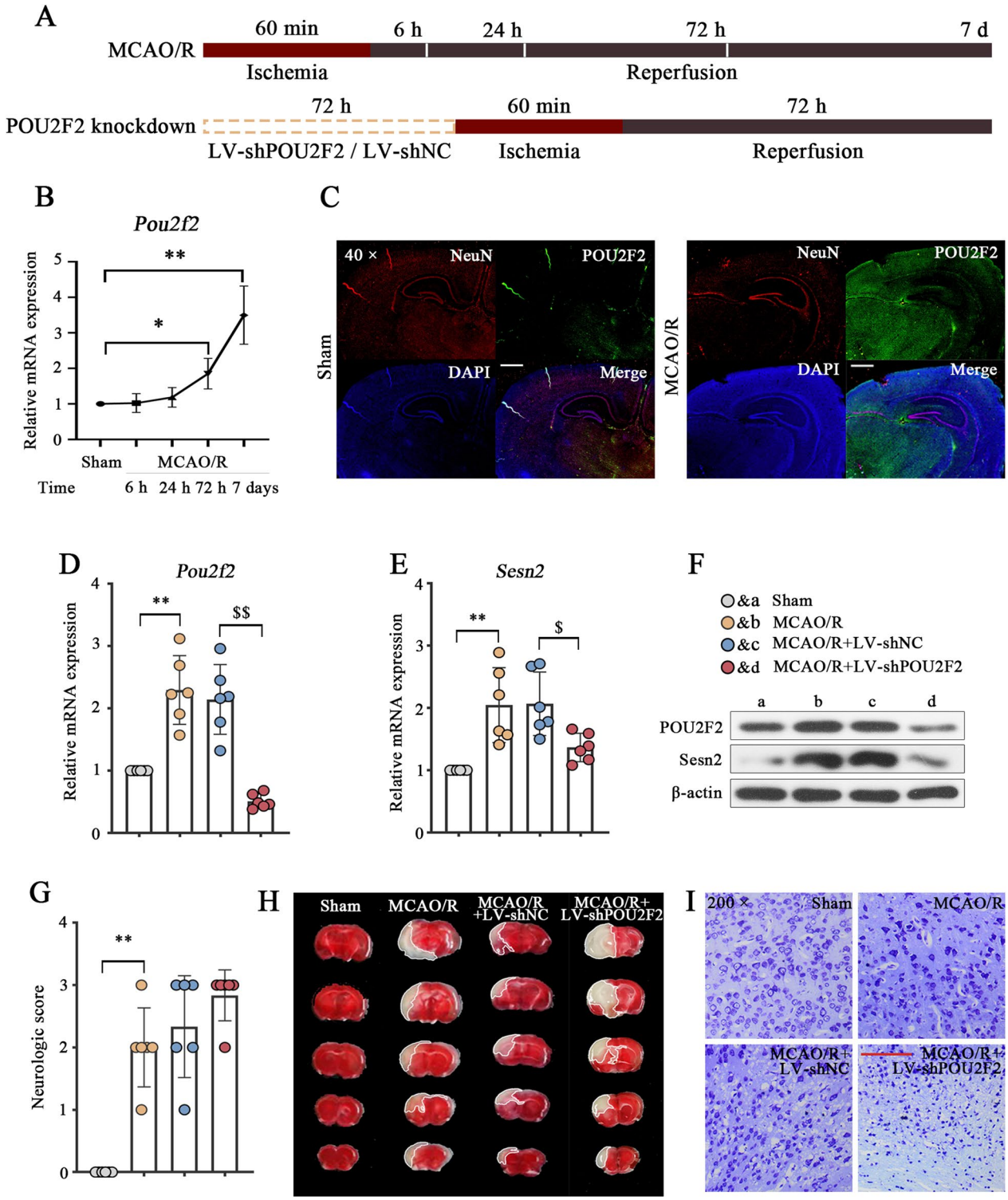

Fig. 1 Depletion of POU2F2 aggravated MCAO/R-induced brain injury in mice. **A** Flow diagrams of animal experiments. **B**POU Class Homeobox 2 (POU2F2) gene expression. $^{*}P<0.05$ vs. Sham, $^{**}P<0.01$ vs. Sham. **C** Representative immunofluorescence images of POU2F2 (green) and neuronal nuclei (NeuN) (red) (scale bar, 500 μm). **D**–**F** The gene (**D**, **E**) and protein (**F**) expression of POU2F2 and Sestrin2 (Sesn2) in ischemic penumbra of cortex. $^{**}P<0.01$ vs. Sham, $^{\$}P<0.05$ vs. MCAO/R + LV-shNC, $^{\$\$}P<0.01$ vs. MCAO/R + LV-shNC. **G** Neurological deficit scores 72 h after MCAO/R. $^{**}P<0.01$ vs. Sham. **H** 2, 3, 5-triphenyltetrazolium chloride (TTC) staining. **I** Nissl staining (scale bar, 100 μm). Results were presented as the means ± standard deviation (SD). *MCAO/R* middle cerebral artery occlusion/reperfusion, *LV-shPOU2F2* POU2F2 short hairpin RNA (shRNA) lentivirus, *LV-shNC* negative control shRNA lentivirus

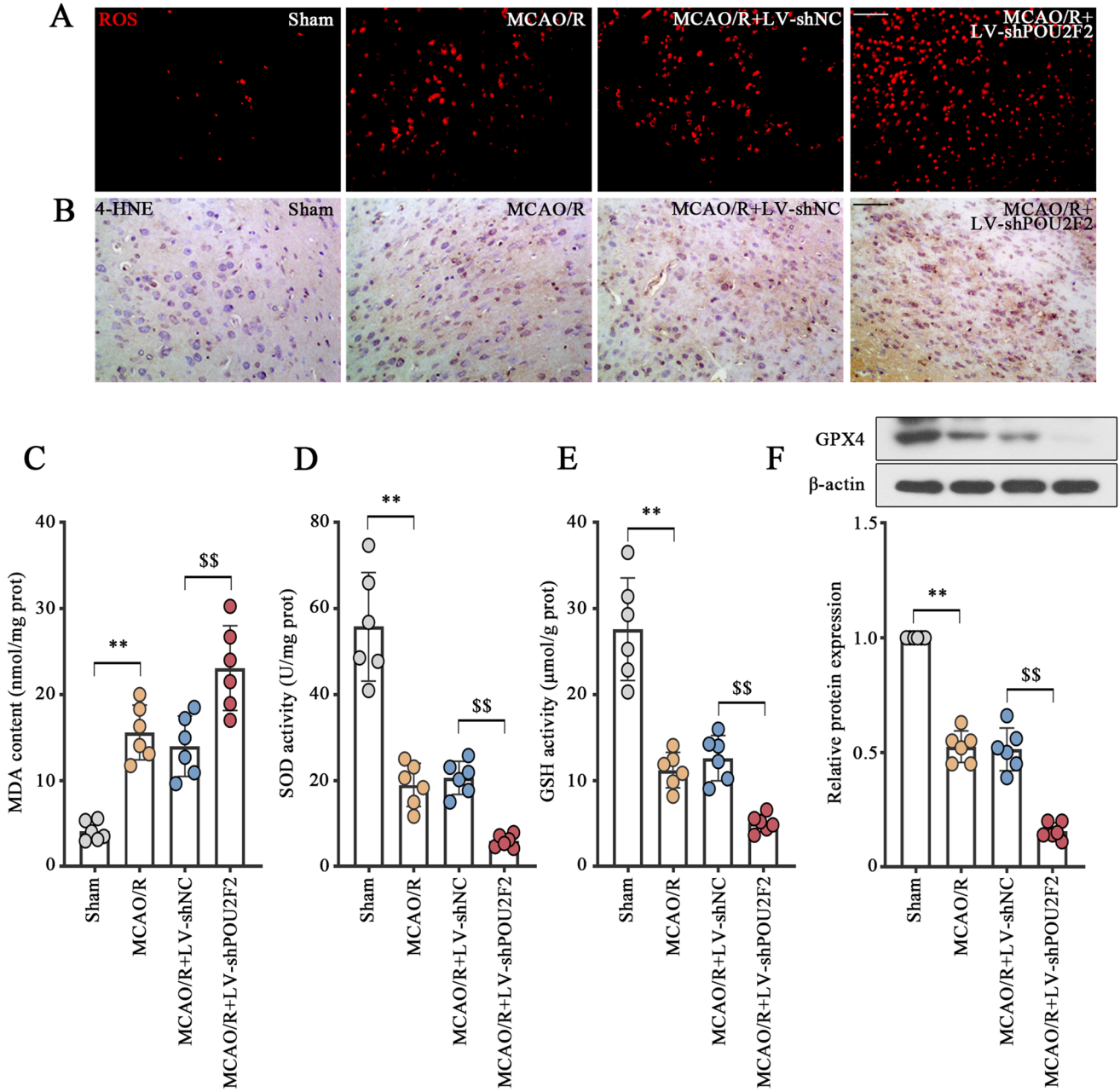

Fig. 2 POU2F2 knockdown aggravated neural oxidative stress and ferroptosis induced by MCAO/R. **A** Reactive oxygen species (ROS) detection by fluorescence staining (scale bar, 50 μm). **B** Immunohistochemistry for 4-hydroxynonenal (4-HNE) (scale bar, 50 μm). **C**–**E** Malondialdehyde (MDA) content **C**, superoxide dismutase (SOD) **D** and glutathione (GSH) **E** activity in ischemic penumbra of cortex. $^{**}P<0.01$ vs. Sham, $^{\$\$}P<0.01$ vs. MCAO/R + LV-shNC. **F** Glutathione peroxidase 4 (GPX4) protein expression. $^{**}P<0.01$ vs. Sham, $^{\$\$}P<0.01$ vs. MCAO/R + LV-shNC. Results were presented as the means ± standard deviation (SD)

increased LDH activity (Fig. 3F). The above results indicated that POU2F2 had impact on neuron survival.

Then we measure oxidative stress and lipid peroxidation in neurons. As shown in Fig. 3H (upper panel), POU2F2 deficiency further exacerbated OGD/R-induced ROS formation in neurons and led to the enhancement of MDA content (Fig. 3G) and the reduction of SOD (Fig. 3I) activity in OGD/R-treated neurons. Lipid ROS was considered the driving force of ferroptosis and is a marker of ferroptosis [11]. IF shown that cellular lipid ROS was markedly increased after treatment with OGD/R (Fig. 3H, lower panel). In POU2F2 knockdown cells, lipid ROS were much more abundant (Fig. 3H, lower panel). Furthermore, OGD/R resulted in decreased GSH activity (Fig. 3J) and

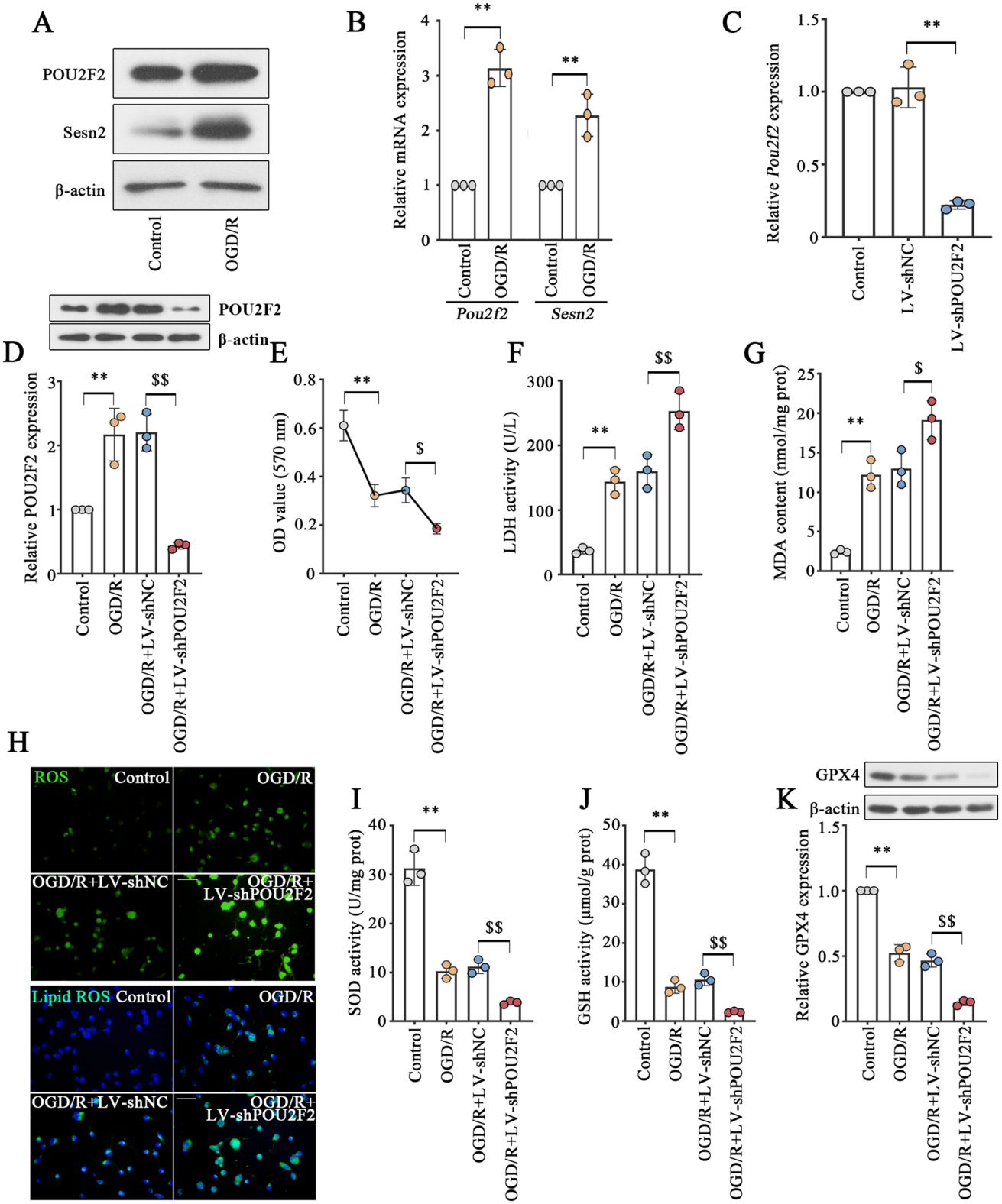
A
POU2F2
Sesn2
β-actin
Control
OGD/R
B
Relative mRNA expression
Control
OGD/R
Pou2f2
Sesn2
C
Relative Pou2f2 expression
Control
LV-shNC
LV-shPOU2F2
POU2F2
β-actin
D
Relative POU2F2 expression
Control
OGD/R
OGD/R+LV-shNC
OGD/R+LV-shPOU2F2
E
OD value (570 nm)
F
LDH activity (U/L)
G
MDA content (nmol/mg prot)
H
ROS
Control
OGD/R
OGD/R+LV-shNC
OGD/R+
LV-shPOU2F2
Lipid ROS
I
SOD activity (U/mg prot)
J
GSH activity (μmol/g prot)
K
GPX4
β-actin
Relative GPX4 expression

◂**Fig. 3** Knockdown of POU2F2 exacerbated neuronal impairment and aggravated oxidative stress and ferroptosis in OGD/R-treated primary neurons. **A**, **B** The protein (**A**) and gene (**B**) expression of POU2F2 and Sesn2. $^{**}P<0.01$ vs. Control. **C** Analysis of POU2F2 transduction efficiency. $^{**}P<0.01$ vs. LV-shNC. **D** POU2F2 protein expression. $^{**}P<0.01$ vs. Control, $^{\$\$}P<0.01$ vs. OGD/R + LV-shNC. **E** Cell viability assay. $^{**}P<0.01$ vs. Control, $^{\$}P<0.05$ vs. OGD/R + LV-shNC. **F** Quantification of lactose dehydrogenase (LDH) release. $^{**}P<0.01$ vs. Control, $^{\$\$}P<0.01$ vs. OGD/R + LV-shNC. **G**MDA content. $^{**}P<0.01$ vs. Control, $^{\$}P<0.05$ vs. OGD/R + LV-shNC. (H) ROS and lipid ROS detection (scale bar, 50 μm). (I-J) SOD (I) and GSH (J) activity. $^{**}P<0.01$ vs. Control, $^{\$\$}P<0.01$ vs. OGD/R + LV-shNC. (K) GPX4 protein expression. $^{**}P<0.01$ vs. Control, $^{\$\$}P<0.01$ vs. OGD/R + LV-shNC. Results were presented as the means ± standard deviation (SD). OGD/R, oxygen–glucose deprivation /reoxygenation

GPX4 expression (Fig. 3K), and the decreases were more noticeable in POU2F2 knockdown neurons (Fig. 3J–K) as compared to control neurons.

POU2F2 Aggravated Oxidative Stress and Ferroptossi via Targeting Sesn2 In Vitro

Sesn2 has been reported to exert a positive role in cerebral injury [20] and it might be the target gene of POU2F2 in bioinformatics websites. The decreased Sesn2 expression was validated in POU2F2 knockdown neurons (Fig. 4A, B). Dual-luciferase reporter and ChIP assays were employed to confirm the interaction between POU2F2 and Sesn2 in HEK-293T cells. Results expounded that POU2F2 overexpression increased the luciferase activity of the different segments of Sesn2 promoter (Fig. 4C). ChIP assay further confirmed that POU2F2 was directly bound to Sesn2 promoter (Fig. 4D), indicating that Sesn2 was the direct transcriptional target of POU2F2. Further, we evaluated whether POU2F2 modulated ferroptosis in the primary neurons under OGD/R condition by targeting Sesn2. Western blot results revealed that Sesn2 overexpression inhibited shPOU2F2-induced the down-regulation of Sesn2 (Fig. 4E). The increased lipid ROS formation induced by POU2F2 deficiency could be abolished by Sesn2 overexpression (Fig. 4F). Silencing POU2F2 increased LDH activity (Fig. 4G) and MDA content (Fig. 4H) and decreased GSH activity (Fig. 4I), which could be reversed by overexpressed-Sesn2 (Fig. 4G–I). The above data suggested that POU2F2 might modulate ferroptosis in the primary neurons induced by OGD/R by targeting Sesn2.

Discussion

In this research, we found a significant induction of POU2F2 expression levels in the ischemic penumbra area 72 h after MCAO/R. Furthermore, the post-CIR induction of POU2F2 protected neurons from oxidative stress and ferropotosis, possibly through binding to Sesn2. Our findings suggested that POU2F2 could be a novel regulator of CIRI. The mechanism diagram was shown in Fig. 5.

MCAO/R model is one of the closest models to mimic human CIRI [36]. Animals experiencing CIR exhibited neuromotor deficits and pathological changes, including brain edema and infarction [37]. In our study, increased neurological deficit scores, infarct areas and neuron loss were observed in mice after MCAO/R, indicating successful induction of CIRI. A previous study reported that POU2F2 was involved in brain development, and that brain injury was accompanied by elevated POU2F2 levels [38]. Besides, Camós et al. [26] reported that POU2F2 was highly expressed in ischemic rat brain cortical slices, which was consistent with our results both in vivo and in vitro. Our research further proved that POU2F2 deficiency intensified MCAO/R-induced above damage indicators, indicating a positive role of POU2F2 in CIRI.

IR injury in the brain is deleterious and leads to the development of certain functional impairments in the body, for instance, impairment of movement and cognition [39]. Ischemic reperfusion injury in the brain includes anomalous production of oxygen free radicals, which may exacerbate the initial ischemic injury[40]. However, it is currently difficult to prevent further oxidative damage caused by reperfusion. Likewise, reperfusion-induced secondary damage is difficult to manage and may leave reversible regions (e.g., penumbra) vulnerable to oxidative damage [41].

Iron is essential for the normal function and activity of neurons. Its overload is involved in the formation of free radicals and causes oxidative damage to neurons. Oxidative stress and lipid peroxidation are two major causes of ferroptosis [11]. The brain is a lipid-rich organ, rendering it highly susceptible to iron-induced lipid hydroperoxidation. There are increasing evidences to emphasize the role of ferroptosis in CIRI [42]. The inhibition of ferroptosis has been proved to be successfully prevented or reduced IR injury in various organs [43]. Research on ferroptosis, nonetheless, is still in its infancy, and there is no simple or accurate method to detect the existence of ferroptosis. Iron overload, diminished antioxidant capacity, and buildup of lipid peroxidation products are generally considered to be the characteristic indicators of ferroptosis [44].

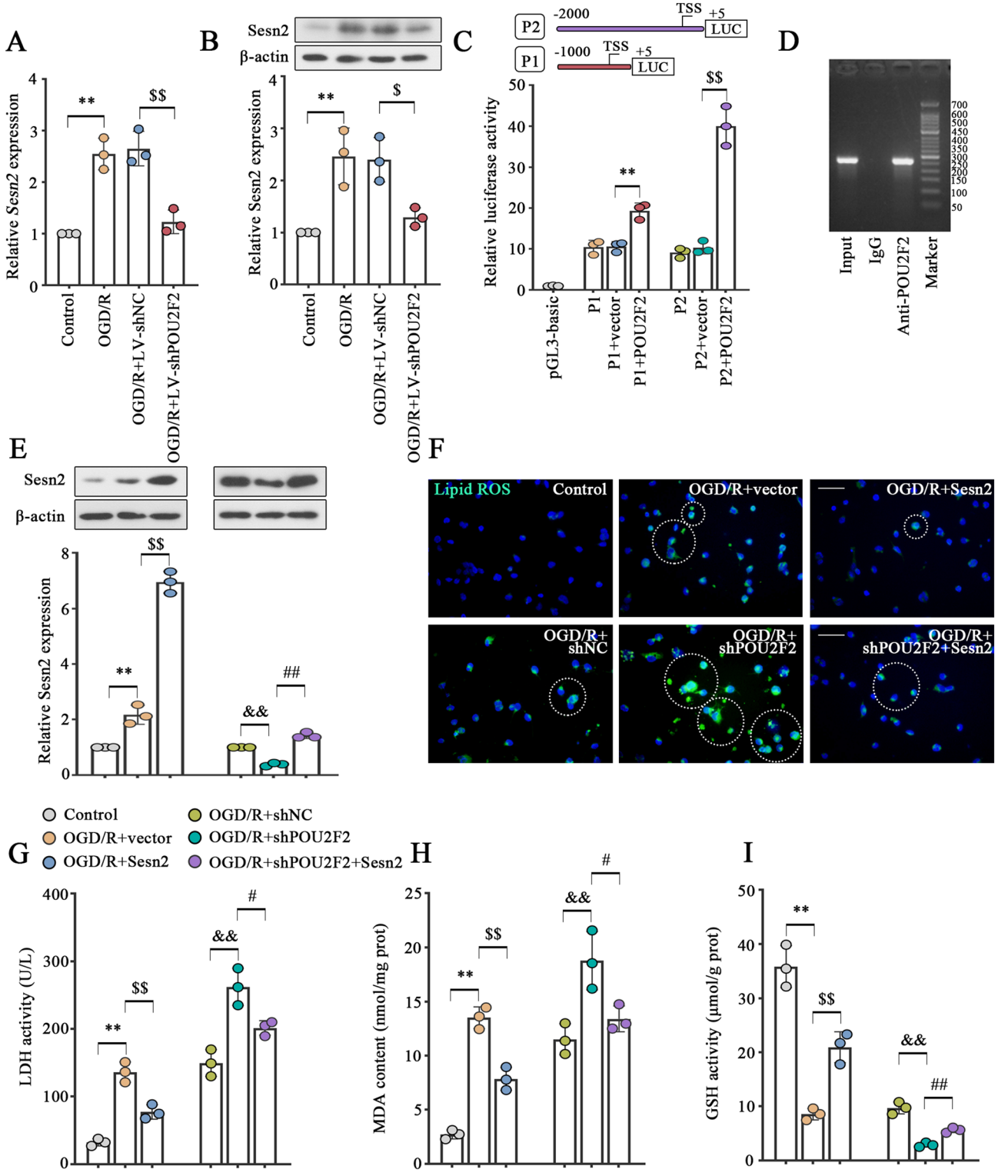

Excess reactive iron provides electrons that generate ROS via the Fenton reaction, promoting lipid peroxidation and triggering ferroptosis [10]. The enrichment of ROS and lipid ROS, 4-HNE and MDA is usually considered to reflect the process of ferroptosis, and SOD and GPX4 are key antioxidant enzymes for scavenging excess ROS and lipid peroxidation [45, 46]. GPX4 serves as a negative regulator of ferroptosis and a central element in lipid peroxide production during ferroptosis at the expense of GSH [12]. It reduced lipid peroxidation and the accumulation of lethal lipid ROS, which are

◂**Fig. 4** POU2F2 aggravated oxidative stress and ferroptossi via targeting Sesn2 in vitro. **A**, **B** The gene (**A**) and protein (**B**) expression of Sesn2. $^{**}P<0.01$ vs. Control, $^{\$}P<0.05$ vs. OGD/R + LV-shNC, $^{\$\$}P<0.01$ vs. OGD/R + LV-shNC. **C** Dual-luciferase assay between the Sesn2 promoter and POU2F2. $^{**}P<0.01$ vs. P1 + vector, $^{\$\$}P<0.01$ vs. P2 + vector. **D** Chromatin immunoprecipitation analysis of POU2F2 binding to Sesn2 promoter. **E** Sesn2 protein expression. $^{**}P<0.01$ vs. Control, $^{\$\$}P<0.01$ vs. OGD/R + vector, $^{\&\&}P<0.01$ vs. OGD/R + shNC, $^{\#\#}P<0.01$ vs. OGD/R + shPOU2F2. **F** Lipid ROS detection by fluorescence staining (scale bar, 50 μm). White circle indicated positive staining. **G** Quantification of LDH release. $^{**}P<0.01$ vs. Control, $^{\$\$}P<0.01$ vs. OGD/R + vector, $^{\&\&}P<0.01$ vs. OGD/R + shNC, $^{\#}P<0.05$ vs. OGD/R + shPOU2F2. **H–I** MDA content (**H**) and GSH activity (**I**). $^{**}P<0.01$ vs. Control, $^{\$\$}P<0.01$ vs. OGD/R + vector, $^{\&\&}P<0.01$ vs. OGD/R + shNC, $^{\#}P<0.05$ vs. OGD/R + shPOU2F2, $^{\#\#}P<0.01$ vs. OGD/R + shPOU2F2. Results were presented as the means ± standard deviation (SD)

the final executions of ferroptosis. Besides, GSH is the also major endogenous antioxidant enzyme [47]. In our research, we proved that MCAO/R or OGD/R treated-mice or primary neurons exhibited hallmark features of oxidative stress and ferroptosis, and confirmed the inhibitory effect of POU2F2. Moreover, in vivo and in vitro experiments, ischemic penumbra in mice and primary neuronal cells with POU2F2 deficiency exhibited more severe neuron damage. These results confirmed our speculation that POU2F2 could ameliorate CIRI by inhibiting oxidative stress and ferroptosis. POU domain family members are considered to be important contributors to cell survival in response to multiple DNA damage. The higher ROS levels were detected in OCT-6 deficiency cells which suggested to respond to enhanced-DNA damage and cell death [48]. This suggested that POU2F2 was upregulated in responded to CIRI, and POU2F2 deficiency might aggravate DNA damage and induce stress, thereby deteriorating CIRI-induced damage.

From bioinformatics analysis, we found that POU2F2 could potentially regulate Sesn2 expression, which was further evidenced by our in vitro experiments. Sesn2 has been reported to play neuroprotective role in some neurodegenerative diseases. Li et al. [20] proved that Sesn2 was highly expressed in CIRI, which was similar to our results and its deficiency aggravated the CIRI. Presently, Sesn2 has been reported to be induced under multiple conditions and protect cells from multiple damages. Previous studies have demonstrated that Sesn2 could protect cells from oxidative stress through the inhibition of ROS accumulation and the promotion of antioxidant enzyme activity [49]. A recent study shown that Sesn2 protected dendrite cells against ferroptosis induced by sepsis [21]. Park et al. [50] reported that Sesn2 could protect against lung injury by inhibiting ferroptosis. As for our research, we verified the protective role of Sesn2 in CIRI by inhibiting ferroptosis. Besides, we further demonstrated that it was regulated by POU2F2, indicating that POU2F2 may aggravate the CIRI progression by mediating Sesn2.

Overall, we certified that POU2F2 was highly expressed in CIRI and its deficiency aggravated the CIRI progression. POU2F2 might bind to the promoter of Sesn2 and start transcription, and then inhibit oxidative stress and ferroptosis to ameliorate CIRI. Our study provided a possible molecular target for CIRI treatment.

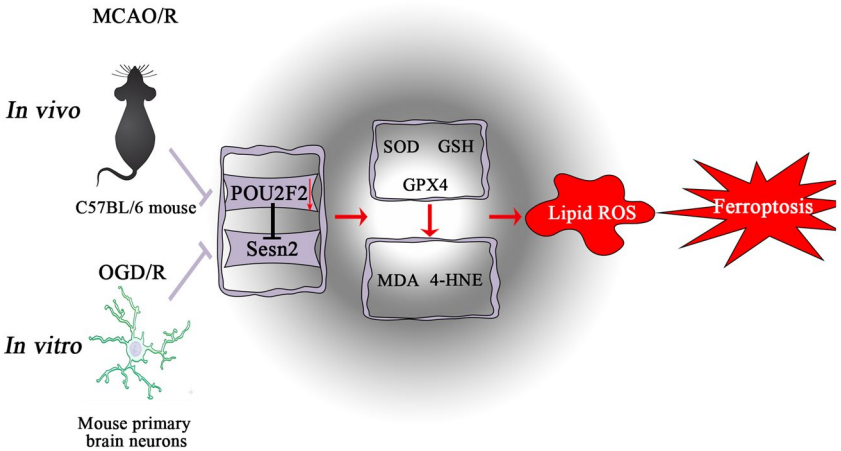

Fig. 5 The mechanism diagram. POU2F2 was upregulated in vivo and in vitro. It protected neurons from oxidative stress ferropotosis by binding to Sesn2

Author Contributions Conceptualization: JY, SY; methodology: JY, QG, LW, SY; writing—original draft preparation: JY; writing—review and editing: SY; funding acquisition: SY.

Funding This research was supported by grants from the Youth Fund Project of National Natural Science Foundation of China (Grant Number 82001226) and the Natural Science Foundation of Jilin Province (Grant Number 20210101357JC).

Data Availability The datasets generated during and/or analyzed during the current study are available from the corresponding author on reasonable request.

Declarations

Conflict of interest The authors have no relevant financial or non-financial interests to disclose.

Ethical Approval The animal experiment in this study was approved by the ethical guideline of the Animal Welfare and Research Ethics Committee of Jilin University.

References

1. Sacco RL, Rundek T (2012) Cerebrovascular disease. Curr Opin Neurol 25(1):1–4. https://doi.org/10.1097/WCO.0b013e32834f89b1
2. Liu W, Wong A, Law AC et al (2015) Cerebrovascular disease, amyloid plaques, and dementia. Stroke 46(5):1402–1407. https://doi.org/10.1161/strokeaha.114.006571
3. Catanese L, Tarsia J, Fisher M (2017) Acute ischemic stroke therapy overview. Circ Res 120(3):541–558. https://doi.org/10.1161/circresaha.116.309278
4. Frizzell JP (2005) Acute stroke: pathophysiology, diagnosis, and treatment. AACN Clin Issues 16(4):421–440 quiz 597-8. https://doi.org/10.1097/00044067-200510000-00002
5. Sanderson TH, Reynolds CA, Kumar R et al (2013) Molecular mechanisms of ischemia-reperfusion injury in brain: pivotal role of the mitochondrial membrane potential in reactive oxygen species generation. Mol Neurobiol 47(1):9–23. https://doi.org/10.1007/s12035-012-8344-z
6. Nagy Z, Nardai S (2017) Cerebral ischemia/repefusion injury: from bench space to bedside. Brain Res Bull. https://doi.org/10.1016/j.brainresbull.2017.06.011
7. Patel RAG, McMullen PW (2017) Neuroprotection in the treatment of acute ischemic stroke. Prog Cardiovasc Dis 59(6):542–548. https://doi.org/10.1016/j.pcad.2017.04.005
8. Meng X, Xie W (2018) Neuroprotective effects of radix scrophulariae on cerebral ischemia and reperfusion injury via MAPK pathways. Molecules. https://doi.org/10.3390/molecules23092401
9. Zhang Y, Zhang Y, Jin XF et al (2019) The role of astragaloside IV against cerebral ischemia/reperfusion injury: suppression of apoptosis via promotion of P62-LC3-autophagy. Molecules. https://doi.org/10.3390/molecules24091838
10. Dixon SJ, Lemberg KM, Lamprecht MR et al (2012) Ferroptosis: an iron-dependent form of nonapoptotic cell death. Cell 149(5):1060–1072. https://doi.org/10.1016/j.cell.2012.03.042
11. Hassannia B, Vandenabeele P, Vanden Berghe T (2019) Targeting ferroptosis to iron out cancer. Cancer Cell 35(6):830–849. https://doi.org/10.1016/j.ccell.2019.04.002
12. Xie Y, Hou W, Song X et al (2016) Ferroptosis: process and function. Cell Death Differ 23(3):369–379. https://doi.org/10.1038/cdd.2015.158
13. Stockwell BR, Friedmann Angeli JP, Bayir H et al (2017) Ferroptosis: a regulated cell death nexus linking metabolism, redox biology, and disease. Cell 171(2):273–285. https://doi.org/10.1016/j.cell.2017.09.021
14. Skouta R, Dixon SJ, Wang J et al (2014) Ferrostatins inhibit oxidative lipid damage and cell death in diverse disease models. J Am Chem Soc 136(12):4551–4556. https://doi.org/10.1021/ja411006a
15. Alim I, Caulfield JT, Chen Y et al (2019) Selenium drives a transcriptional adaptive program to block ferroptosis and treat stroke. Cell 177(5):1262–1279
16. She X, Lan B, Tian H et al (2020) Cross talk between ferroptosis and cerebral ischemia. Front Neurosci 14:776. https://doi.org/10.3389/fnins.2020.00776
17. Budanov AV, Lee JH, Karin M (2010) Stressin' Sestrins take an aging fight. EMBO Mol Med 2(10):388–400. https://doi.org/10.1002/emmm.201000097
18. Pasha M, Eid AH (2017) Sestrin2 as a novel biomarker and therapeutic target for various diseases. Oxid Med Cell Longev. https://doi.org/10.1155/2017/3296294
19. Wang P, Zhao Y, Li Y et al (2019) Sestrin2 overexpression attenuates focal cerebral ischemic injury in rat by increasing Nrf2/HO-1 pathway-mediated angiogenesis. Neuroscience 410:140–149. https://doi.org/10.1016/j.neuroscience.2019.05.005
20. Li L, Xiao L, Hou Y et al (2016) Sestrin2 silencing exacerbates cerebral ischemia/reperfusion injury by decreasing mitochondrial biogenesis through the AMPK/PGC-1α pathway in rats. Sci Rep 6:30272. https://doi.org/10.1038/srep30272
21. Li JY, Ren C, Wang LX et al (2021) Sestrin2 protects dendrite cells against ferroptosis induced by sepsis. Cell Death Dis 12:834. https://doi.org/10.1038/s41419-021-04122-8
22. Staudt LM, Clerc RG, Singh H et al (1988) Cloning of a lymphoid-specific cDNA encoding a protein binding the regulatory octamer DNA motif. Science 241(4865):577–580. https://doi.org/10.1126/science.3399892
23. Hodson DJ, Shaffer AL, Xiao W et al (2016) Regulation of normal B-cell differentiation and malignant B-cell survival by OCT2. Proc Natl Acad Sci USA 113(14):E2039–E2046. https://doi.org/10.1073/pnas.1600557113
24. Latchman DS (1996) The Oct-2 transcription factor. Int J Biochem Cell Biol 28(10):1081–1083. https://doi.org/10.1016/1357-2725(96)00050-7
25. Latchman DS (1996) Activation and repression of gene expression by POU family transcription factors. Philos Trans R Soc Lond B 351(1339):511–515. https://doi.org/10.1098/rstb.1996.0049
26. Camós S, Gubern C, Sobrado M et al (2014) Oct-2 transcription factor binding activity and expression up-regulation in rat cerebral ischaemia is associated with a diminution of neuronal damage in vitro. Neuromolecular Med 16(2):332–349. https://doi.org/10.1007/s12017-013-8279-1
27. Lelièvre E, Lionneton F, Soncin F et al (2001) The Ets family contains transcriptional activators and repressors involved in angiogenesis. Int J Biochem Cell Biol 33(4):391–407. https://doi.org/10.1016/s1357-2725(01)00025-5
28. Ikeshima H, Imai S, Shimoda K et al (1995) Expression of a MADS box gene, MEF2D, in neurons of the mouse central nervous system: implication of its binary function in myogenic and neurogenic cell lineages. Neurosci Lett 200(2):117–120. https://doi.org/10.1016/0304-3940(95)12092-i
29. Crack PJ, Taylor JM (2005) Reactive oxygen species and the modulation of stroke. Free Radic Biol Med 38(11):1433–1444. https://doi.org/10.1016/j.freeradbiomed.2005.01.019

30. Li M, Ma Y, Zhong Y et al (2020) KALRN mutations promote antitumor immunity and immunotherapy response in cancer. J ImmunoTher Cancer. https://doi.org/10.1136/jitc-2019-000293
31. McCullough LD, Blizzard K, Simpson ER et al (2003) Aromatase cytochrome P450 and extragonadal estrogen play a role in ischemic neuroprotection. J Neurosci 23(25):8701–8705. https://doi.org/10.1523/jneurosci.23-25-08701.2003
32. Chen F, Zhang L, Wang E et al (2018) LncRNA GAS5 regulates ischemic stroke as a competing endogenous RNA for miR-137 to regulate the Notch1 signaling pathway. Biochem Biophys Res Commun 496(1):184–190. https://doi.org/10.1016/j.bbrc.2018.01.022
33. Li X, Xia Q (2021) Annexin-A1 SUMOylation regulates microglial polarization after cerebral ischemia by modulating IKKα stability via selective autophagy. Sci Adv. https://doi.org/10.1126/sciadv.abc5539
34. Liu H, Li Y, Sun S et al (2021) Catalytically potent and selective clusterzymes for modulation of neuroinflammation through single-atom substitutions. Nat Commun 12:114. https://doi.org/10.1038/s41467-020-20275-0
35. Conrad M, Angeli JP, Vandenabeele P et al (2016) Regulated necrosis: disease relevance and therapeutic opportunities. Nat Rev Drug Discov 15(5):348–366. https://doi.org/10.1038/nrd.2015.6
36. Longa EZ, Weinstein PR, Carlson S et al (1989) Reversible middle cerebral artery occlusion without craniectomy in rats. Stroke 20(1):84–91. https://doi.org/10.1161/01.str.20.1.84
37. Guo P, Jin Z, Wu H et al (2019) Effects of irisin on the dysfunction of blood-brain barrier in rats after focal cerebral ischemia/reperfusion. Brain Behav 9(10):e01425. https://doi.org/10.1002/brb3.1425
38. Bakheet SA, Basha MR, Cai H et al (2007) Lead exposure: expression and activity levels of Oct-2 in the developing rat brain. Toxicol Sci 95(2):436–442. https://doi.org/10.1093/toxsci/kfl163
39. Gottesman RF, Hillis AE (2010) Predictors and assessment of cognitive dysfunction resulting from ischaemic stroke. Lancet Neurol 9(9):895–905. https://doi.org/10.1016/s1474-4422(10)70164-2
40. Sun MS, Jin H, Sun X et al (2018) Free radical damage in ischemia-reperfusion injury: an obstacle in acute ischemic stroke after revascularization therapy. Oxid Med Cell Longev. https://doi.org/10.1155/2018/3804979
41. Pan J, Konstas AA, Bateman B et al (2007) Reperfusion injury following cerebral ischemia: pathophysiology, MR imaging, and potential therapies. Neuroradiology 49(2):93–102. https://doi.org/10.1007/s00234-006-0183-z
42. Wang P, Cui Y, Ren Q et al (2021) Mitochondrial ferritin attenuates cerebral ischaemia/reperfusion injury by inhibiting ferroptosis. Cell Death Dis 12:447. https://doi.org/10.1038/s41419-021-03725-5
43. Li X, Ma N, Xu J et al (2021) Targeting ferroptosis: pathological mechanism and treatment of ischemia-reperfusion injury. Oxid Med Cell Longiv. https://doi.org/10.1155/2021/1587922
44. Li N, Wang W, Zhou H et al (2020) Ferritinophagy-mediated ferroptosis is involved in sepsis-induced cardiac injury. Free Radic Biol Med. https://doi.org/10.1016/j.freeradbiomed.2020.08.009
45. Yamada N, Karasawa T, Kimura H (2020) Ferroptosis driven by radical oxidation of n-6 polyunsaturated fatty acids mediates acetaminophen-induced acute liver failure. Cell Death Discov 11:144. https://doi.org/10.1038/s41419-020-2334-2
46. Galaris D, Barbouti A, Pantopoulos K (2019) Iron homeostasis and oxidative stress: an intimate relationship. Biochim Biophys Acta Mol Cell Res 1866(12):118535. https://doi.org/10.1016/j.bbamcr.2019.118535
47. Cao JY, Dixon SJ (2016) Mechanisms of ferroptosis. Cell Mol Life Sci 73(11–12):2195–2209. https://doi.org/10.1007/s00018-016-2194-1
48. Fionda C, Di Bona D, Kosta A et al (2019) The POU-domain transcription factor Oct-6/POU3F1 as a regulator of cellular response to genotoxic stress. Cancers (Basel). https://doi.org/10.3390/cancers11060810
49. Budanov AV, Sablina AA, Feinstein E et al (2004) Regeneration of peroxiredoxins by p53-regulated sestrins, homologs of bacterial AhpD. Science 304(5670):596–600. https://doi.org/10.1126/science.1095569
50. Park SJ, Cho SS, Kim KM et al (2019) Protective effect of sestrin2 against iron overload and ferroptosis-induced liver injury. Toxicol Appl Pharmacol. https://doi.org/10.1016/j.taap.2019.114665